Superluminal Maxwell Displacement Current measured in the near-field of a spherical capacitor

Emmanouil N. Markoulakis[1*], William D. Walker[2], Emmanuel Antonidakis[1]

[1]*Computer Technology Informatics & Electronic Devices Lab, Department of Electronic Engineering, Hellenic Mediterranean University, Romanou 3, Chania 73133, Crete, Greece.*

[2]*William D. Walker, University of Freiburg IMTEK, Georges-Köhler-Allee 103, 79108 Freiburg, Germany.*

[*]*Corresponding Author E-mail: markoul@hmu.gr*

Abstract

We report herein the observed null or negative results in measuring any known finite light speed in air, of the one way near-field signal and information velocity, of the field displacement current between the poles of a total 1.5m separated poles spherical air capacitor, caused by its impulse spark discharge.

Keywords: Displacement current, capacitor, near-field, speed of light, superluminal, non-local

1. Introduction

According to Maxwell's classical electromagnetic theory, a field displacement current exists between the conductive plates or poles of every capacitor. It's important to note that this current is not the same as an electron current. The displacement current is responsible for pushing the charges in an electric circuit that exists on the poles of a capacitor. This electric field observed between the poles of a capacitor acts effectively as a displacement charge current, shifting electric charges traveling from one pole to the other. Even if there is an electric insulating dielectric like air in-between these poles, the displacement current continues to operate. For a better understanding, you can refer to Figure 1.
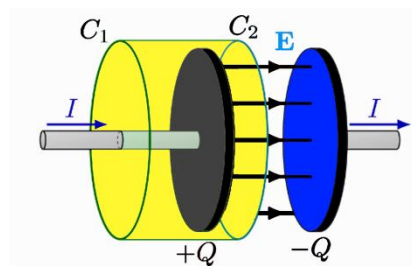

Fig. 1 Field Displacement Current between the plates of an air capacitor responsible for pushing the charges in an electric circuit between the plates of the capacitor.

$$I_{\mathrm{D}} = \iint_S \mathbf{J}_{\mathrm{D}} \cdot \mathrm{d}\mathbf{S} = \iint_S \frac{\partial \mathbf{D}}{\partial t} \cdot \mathrm{d}\mathbf{S} = \frac{\partial}{\partial t}\iint_S \mathbf{D} \cdot \mathrm{d}\mathbf{S} = \frac{\partial \Phi_{\mathrm{D}}}{\partial t}. \tag{1}$$

As per Equation (1), the current associated with the displacement field I_{D} observed during the charging or discharging of a capacitor is equal to the rate of change of electric flux Φ_{D} within the electric field E present between the capacitor plates. This means that any sudden change in the electric displacement field E, as shown in Figure 1, caused by charging or discharging the capacitor, will propagate between the poles of the capacitor as a signal moving at the speed of light.

Note that the current fluctuation or signal in the displacement field will produce both electromagnetic wave radiation and longitudinal scalar field fluctuation components. You can observe this phenomenon in Figure 1, where you can see parallel straight electric flux lines between the plates of a capacitor. The force is aligned with the Poynting energy transfer vector, similar to pressure vectors in an acoustic longitudinal wave or water tsunami.

According to the theory of special relativity, a short-range Coulomb electric longitudinal fluctuation is believed to travel at the speed of light between the plates of a capacitor in the far-field. This means that if the separation of the plates is multiple times the wavelength spectrum of the electrostatic field's impulse charge or discharge signal, it should be possible to observe this phenomenon. However, it has not been experimentally proven to be the case for the near-field, where the separation of the capacitor plates is less than one wavelength. This is typically the case for capacitors in wired electric circuits. Therefore, most displacement fields that exist between the poles of electronic capacitor devices should be regarded as near-field interactions. The motivation for our experiment is due to the research conducted by Walker W. et al. from 1997 to 2023 [1] [2] [3] [4]. Their research showed that, contrary to Relativity, electromagnetic waves propagate instantaneously in the near-field and reduce to the speed of light about one wavelength from the source when transmitted between a Tx and Rx dipole antenna pair. In our experiment, we hypothesize that the superluminal effect being studied is due to the longitudinal field component transmitted within one wavelength in the near-field between the transmitter signal source Tx and the receiver Rx. This field component dies off very quickly within one wavelength distance range, and then the transverse EM wave continues its path at normal light speed for the specific medium or else speed c in a vacuum.

In addition to the aforementioned observations, Maxwell's theory and the equations themselves predict an instantaneous propagation time for the displacement current, rendering it non-local in nature (see "Results and Discussion" section). Since our experiment operated in the near-field, the observed effect could potentially be characterized as a superluminal signal, although it is important to note that the term "non-local" typically refers to phenomena in the far-field and does not imply the transmission of information.

Next we will present a novel table-top experiment and its results which specifically are focused to measure the longitudinal energy component of the displacement current of an air capacitor in the near-field propagation speed between its two poles.

2. Apparatus and Methods

2.1 Experiment setup

Our experiment setup is based on a previous independent experiment by W.G. Gasser [5] which nevertheless differs with our setup, the theoretical background we present, the measurement method that is used and results. Which measured a finite speed two to five times the speed of light c in the near-field opposite to our experiment which reports a null or negative result unable to measure the known speed of light on air around 1.0003 times slower than the speed of light c in the vacuum free space. Therefore, an instantaneous propagation speed reported or at least consequently depending the time resolution technical specification limits of our measuring apparatus, superluminal propagation speed many more times the speed of light c in the vacuum in the near-field. Our setup is shown in Figure 2:
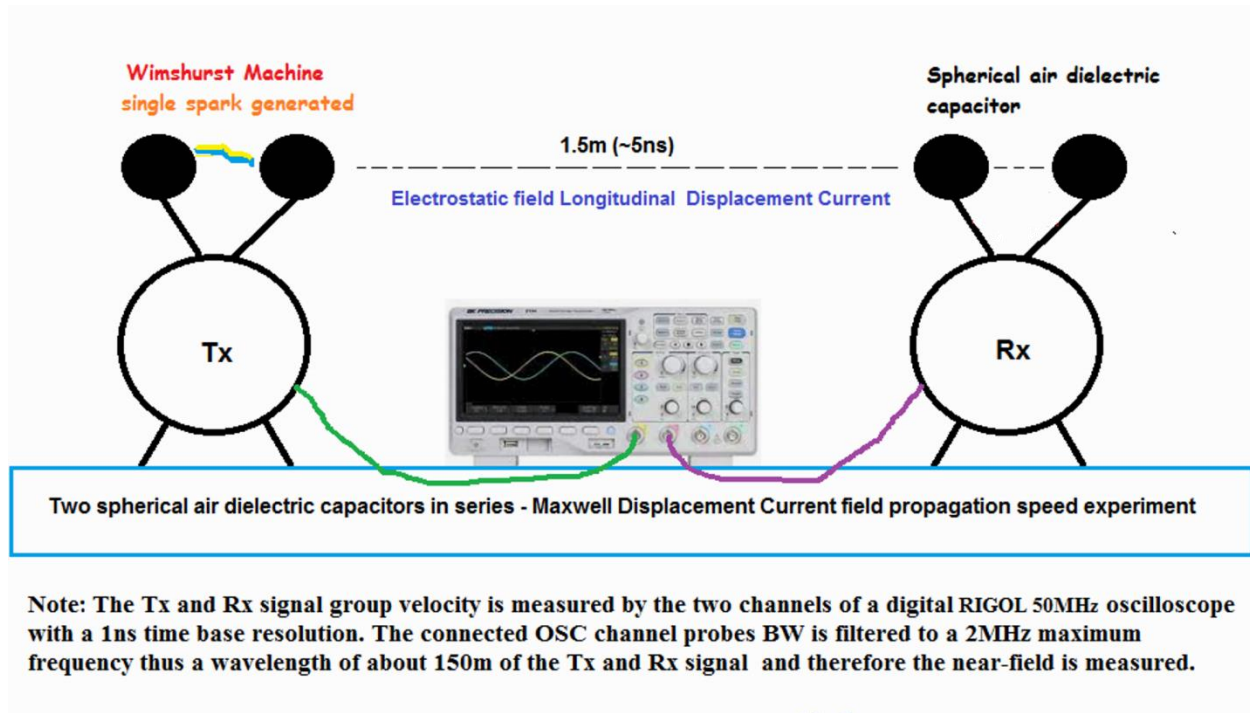

Fig. 2 Experiment setup and apparatus for the displacement current propagation signal speed measurement.

The Tx spark gap spherical capacitor of the Wimshurst machine shown in Figure 3(a) is aligned in series with the Rx capacitor shown in Figure 3(b), with a separation of 1.5m or approximately 5ns light nanoseconds based on the speed of light c in a vacuum. Together, they form a single capacitor with a separation of 1.5m between its poles. This distance is significant and allows for the necessary

delay to enable the oscilloscope to measure the speed of the signal. The oscilloscope has a maximum resolution of 1 nanosecond per sub-division, and the cursors can step in 400 picoseconds increments. The electric spark discharge arc generated in the air at the Tx capacitor (i.e. spark gap) of the Wimshurst machine is aligned longitudinally using a laser with the Rx capacitor, ensuring that the maximum signal amplitude of the longitudinal impulse component is received and measured.

The electric spark that is aligned generates a displacement current by discharging the previously charged direct current (d.c.) capacitors of the transmitter (Tx) and the receiver (Rx), forming a total capacitance. The predicted longitudinal fluctuation signal component of the electric field with a propagation time delay of 5ns light nanoseconds based on the speed of light c in a vacuum, can be measured in the near-field by comparing the signals displayed on the two oscilloscope channels.

The oscilloscope probe on the Tx spark generator is not touching the two spheres of the spark gap. Instead, a classic dipole antenna is used underneath the spark gap in close proximity to sample the signal. This ensures that the electric arc generation is not disturbed by the proximity of the oscilloscope probe, which could potentially damage the oscilloscope. The generator produces at least 30KV/cm voltage before it discharges. The Tx probe is connected to the dipole antenna, which, even though it is isolated, it is able to pick up the induced impulse signal in the range of a few volts.
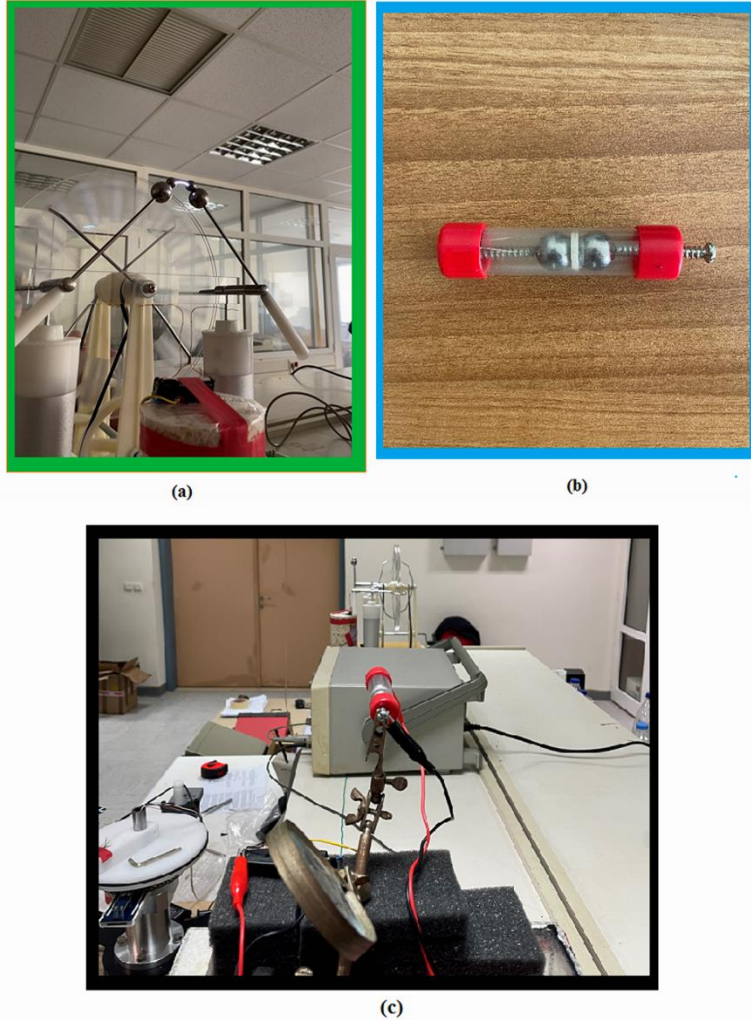
Fig.3 (a) Electric discharge spark arc generated and signal sampled with the dipole antenna 10cm underneath (b) The Rx capacitor using a 2mm ring spacer. The two spheres used are neodymium 1cm diameter magnets used to ease the installation (c) Photograph of the whole table-top lab experiment setup. The oscilloscope in the center is not the actual one used in the experiment and was later on replaced with a RIGOL DS1052E 50MHz 1Gsps.

The Rx osc probe was in electrical contact with the Rx spherical magnet capacitor. The air dielectric thickness of the Rx capacitor is 2mm, and the spark gap in the Tx is 8mm. Both ch1 and ch2 input probes of the oscilloscope are each connected in parallel with a 1.5Vdc battery bias for trigger level reference and random low frequency noise compression. Also, it is very important for this experiment that the Rx spherical magnet capacitor sensor Fig. 3(b) to be pre-charged at 1.5Vdc bias voltage before spark generation occurs.

An electric discharge spark emits a frequency spectrum that includes mainly blue visible light and invisible UV. It has been experimentally confirmed that it also generates radio frequencies, which can range from 150 KHz up to 30 GHz, although they are more commonly found in the range of 150 KHz to 10 MHz. [6]

The signal from both Tx and Rx detectors is passed through a RC low-pass filter circuit, before they are sent onto the Oscilloscope for measurement, as shown in Figure 4. The cut-off frequency of the filter is set to about 2 MHz for both filters in order to reduce the bandwidth of both the transmitter

(Tx) and receiver (Rx) signals. This helps to limit the frequency dispersion distortion effect on the Rx signal caused by the non-linear near-field (refer to the Phase vs. kr graph in Figure 11) and indoor reflections. At the same time, it ensures that only near-field frequencies are measured by the oscilloscope probes, while far-field frequencies do not interfere with the signal group velocity measurement. This is important because the Rx signal should be as less distorted as possible compared to the Tx signal in order for the impulse signal group velocity measurement to be reliable. We did not use the internal built-in oscilloscope filters because we wanted the filtering and bias to happen as close as possible to the Tx and Rx sensors.
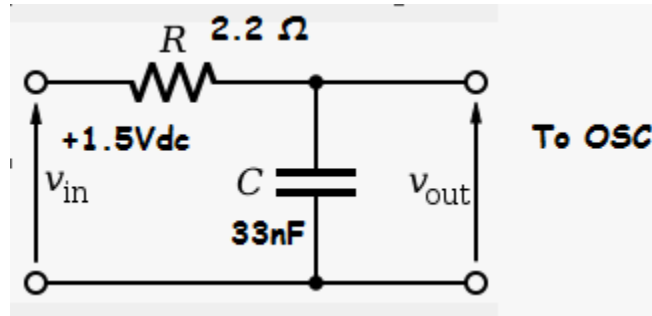

Fig. 4 LPF circuit schematic used for each of the oscilloscope probes. The filter is d.c. biased at 1.5 Volts

 The maximum probed frequency for the experiment setup mentioned above is 2MHz. At this frequency, the near-field ratio is calculated as $r/\lambda=1.5/150=0.01$, which means that the wavelength is 100 times larger than the distance between transmitter Tx and receiver Rx. This puts us inside the very near-field, where we hypothesize that a longitudinal superluminal capacitor displacement current field exists. According to our theory, any signal for charge or discharge impulse is instantaneously transmitted (i.e. superluminally) between the two parallel plates of the total capacitor's 1.5m in length, air inner space.

 The aim of this experimental setup is to measure the speed of charge displacement current signal propagation between the inner-space field of a 1.5-m dielectric capacitor filled with air. The objective is to demonstrate that the longitudinal field displacement current between the plates of an air or vacuum capacitor has an impulse signal speed (i.e. group velocity) that is practically instantaneous, which is faster than the speed of light. This would prove that Maxwell's theory is correct about a non-local displacement current, and that superluminal signal transmission is possible in the near-field.

 In the experiment setup, both ch1 and ch2 probes of the oscilloscope (referred to as osc for short) are positioned horizontally polarized and aligned with the dotted line shown in the illustration of Figure 2. This is done to probe only the longitudinal displacement field capacitor current caused by the electric discharge arc spark created at the spark gap. Oscilloscope ch1 probing Tx will be used to trigger latching on both ch1 and ch2 channels so that both the Tx and Rx signal waveforms can be held off and displayed for comparison of the time delay. We are dealing with single impulses of finite duration, not continuous signals, so we'll measure the group velocity of the two impulses Tx and Rx time delay, not the phase velocity of continuous planar signals. Both impulse signals are measured at their rise phase front. We expect indoor reflections interference to be minimized because of the single-shot impulse nature of this experiment and no continuous signal used. The oscilloscope holdoff time is set at 1.5s to further reduce incoming environment reflections received and possible interfering with the measurement. The complete set of settings used for the oscilloscope during the

experiment, and also charging procedure of the Wimshurst machine can be found here[1]. In general, the maximum allowed measured signal propagation time and minimum speed by which Einstein's absolute speed c of light is verified is 4-5ns, leaving a small 1ns experiment uncertainty margin. Any other result obtained less than 4ns will be characterized as a null result and instantaneous, superluminal signal propagation in the near-field observed. This is considered a control experiment, and we believe that no less than 4ns measured is possible for a conventional physics explanation. The entire experiment setup and apparatus are displayed in Fig. 3(c). We conducted three 8mm spark gap runs of the experiment with three spark measurements on each run and three runs on a 30mm spark gap setting.

2.2 Balancing the Tx and Rx wired Oscilloscope channels

 To ensure the credibility of the experiment and the accuracy of the task, it is crucial to balance the two wired measuring paths, ch1 and ch2, which are connected with the Tx and Rx signals. We conducted several control experiments to make sure that these two paths have identical and systematic time delay differences of less than 1ns. This was done to measure the spark radiation propagation speed traveling the 1.5m straight path distance and compare it to 5ns time delay due to the speed of light c predicted by Relativity. To transmit the signal to the oscilloscope, a 1.5 meter-long 50 ohm coaxial cable is used. At the other end, simple insulated wire with crocodile clips is attached, adding another 25 centimeters. There is also a 10-centimeter air travel distance between the dipole antenna sensor and the spark gap. All in all, the total distance of the Tx path from the spark gap to CH1 of oscilloscope is 1.85 meters. The path from the sensor to CH2 of the oscilloscope for the Rx is made up of a 1.5m coaxial 50-ohm cable and a 33cm simple wire, totaling 1.83m. The length of the Rx channel wired osc path is made intentionally 2cm less than the length of the Tx osc path to compensate for the fact that the Tx osc signal travels 10cm on air from the spark gap to the dipole antenna positioned underneath, which is not the case for the Rx osc signal that travels solely on wire (i.e. speed of light on air is faster than the speed of light on an insulated wire). Both osc channels are filtered using a low-pass RC filter with a cut-off frequency of 2MHz, which is measured at both filters.

 In Figure 5, we present two block diagrams. The first one, shown in Figure 5(a), depicts the standard setup of the experiment. The second one, shown in Figure 5(b), illustrates the configuration used for the control experiment. The latter was designed to identify any potential imbalance in the transmission (Tx) and reception (Rx) wired path of the experiment leading to the oscilloscope. The

---

[1] http://tinyurl.com/bddhytvs

block diagrams in Figure 5 also provide an approximation of the actual cable lengths used in the experiments.
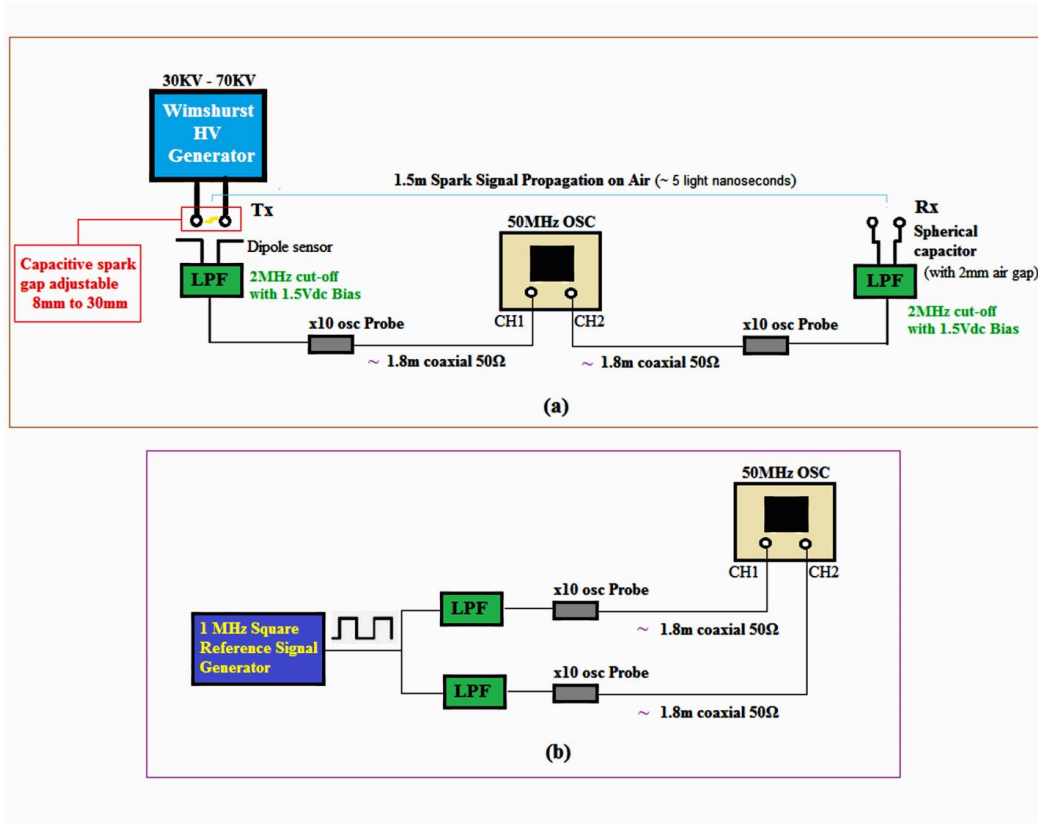

Fig. 5 (a) Block diagram of the experiment setup (b) Block diagram of the control balance experiment.

Two coaxial probe oscilloscope cables with identical length of 1.5m and impedance of 50-Ω were used, along with a simple extension insulated wire with clips as previously described. A square wave reference signal of 1MHz was employed to detect any imbalance existing between the total wired path of both channels, including their low-pass filters that were connected.
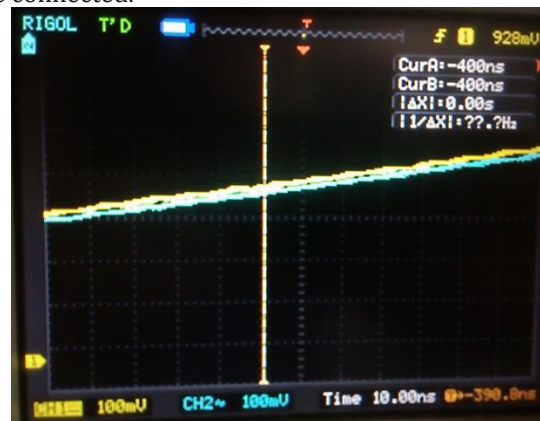

Fig. 6 Imbalance measurement of the Tx (yellow) and Rx (white) osc wired paths including the connected LPFs.

In Figure 6, we can see the most accurate measurement we could achieve with our oscilloscope. The two total wired channels, Tx and Rx, including the LPFs, were measured with a 10ns/DIV time base scale of the oscilloscope and were found to match. The yellow top line represents the Tx ch1, and the

blue bottom line represents the Rx ch2. We visually estimate an uncertainty of 1ns from Figure 6 for a reference square signal of 1MHz. In Figure 7, we have measured the actual imbalance we estimated previously, with the Tx ch1 leading the Rx ch2 by 1.2ns. This measurement is very close to the uncertainty of our experiment, which we set at 1ns.
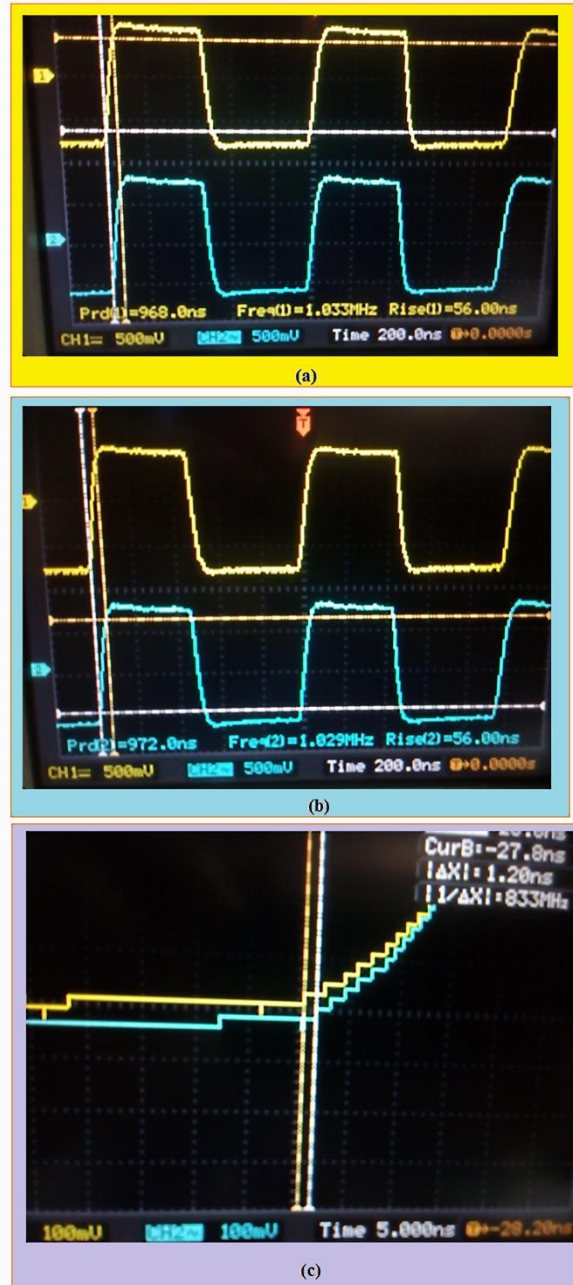

Fig. 7 (a) (b) CH1:Tx & CH2:Rx injected 1MHz reference signal and their measured parameters (c) A 1.2ns measured imbalance between Tx (faster) and Rx wired paths including their LPFs very close to the uncertainty limit set for the experiment of 1ns

 The small maximum imbalance found during the control experiment may have been caused by the random fluctuations of the continuous square signal that was injected from the generators to the two

channels. However, this finding will not affect the conclusions of the single-shot actual experiment, which had an uncertainty set at 1ns to cover any unknown parameters such as the characteristics of the Tx and Rx sensors. We confirmed this through the actual experiment with the sensors connected, and in all our measurements, we couldn't detect any delay between the transmit Tx and receive Rx spark signal. To be thorough, we also swapped the wiring, probes, and low-pass filters connected to the two ch1 and ch2 inputs of the oscilloscope and obtained the same null result time difference between the Tx and Rx signals.
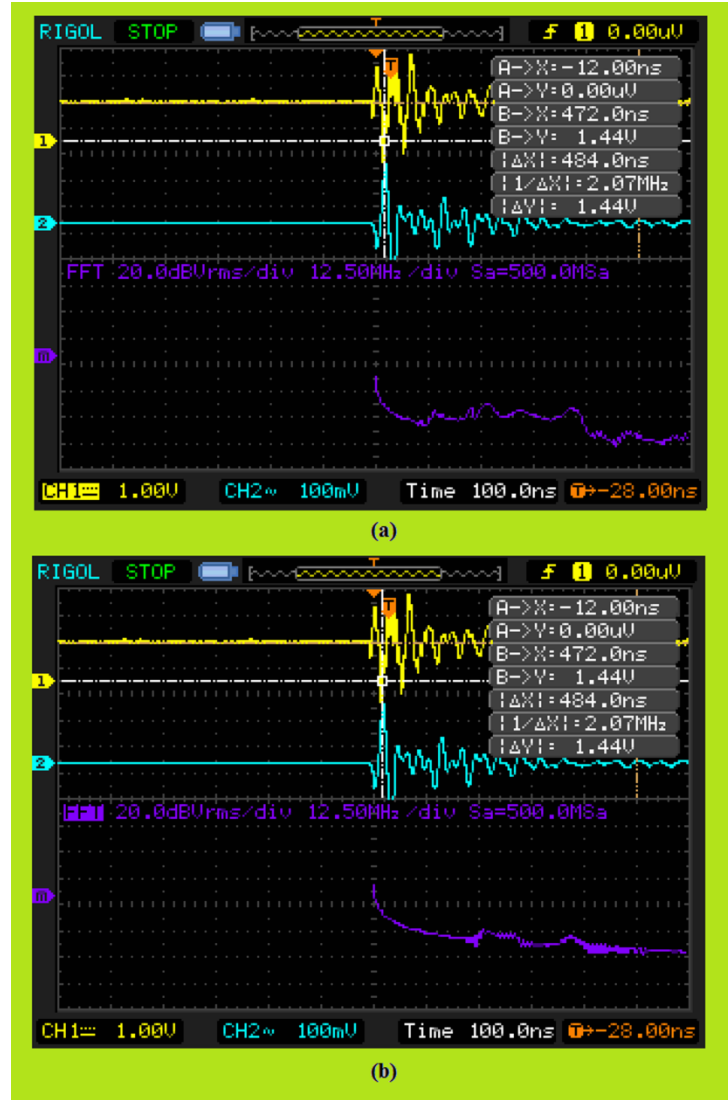

Fig. 8 The Fourier analysis transforms of the Tx and Rx filtered spark signal measured, both showing similar harmonics content and spectrum peaking at a dominant harmonic of approximate 2MHz. (a) FFT of Tx signal (b) FFT of Rx signal.

In Figure 8(a) and 8(b), we compared the Fourier analysis harmonics spectrum of the transmit (Tx) and receive (Rx) signals of a spark signal that we generated during the experiment. We found similar harmonics content and a dominant harmonic frequency in both signals at 2MHz. This ensures that the signals and information contained are suitable for comparison in our experiment. Additionally, it

ensures that the receive signal is not heavily altered by reflections or other phenomena that could interfere with the experiment.

3. Results and Discussion

In our measurements, we found no detectable time delay between Tx and Rx signals down to the 1ns time scale. Fig. 9 & 10 show a small sample of these results (additional sample in footnote 1).
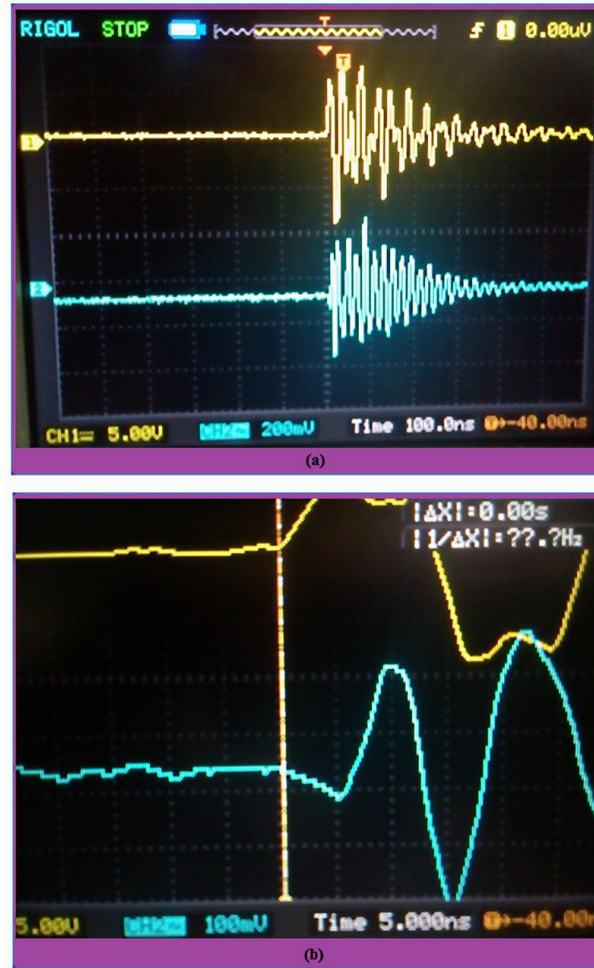

Fig. 9 (a) Tx (yellow, top) and Rx (blue, bottom) signals generated by the electric spark discharge shown at 100ns/DIV time osc base (b) The Tx (yellow, top) and Rx (blue, bottom) signals previously shown in Fig. 9(a), measured at the 5ns/DIV time osc base with 1ns visible sub-divisions.

In figure 9(b), we used the oscilloscope's two vertical cursors, yellow for ch1 and the Tx signal, and white for ch2 and the Rx signal. The cursors were placed together with a 400 picoseconds step resolution during the measurement. We determined that no time difference of the rise phase front of the two impulse signals could be measured due to the time resolution limitations of this particular oscilloscope model.
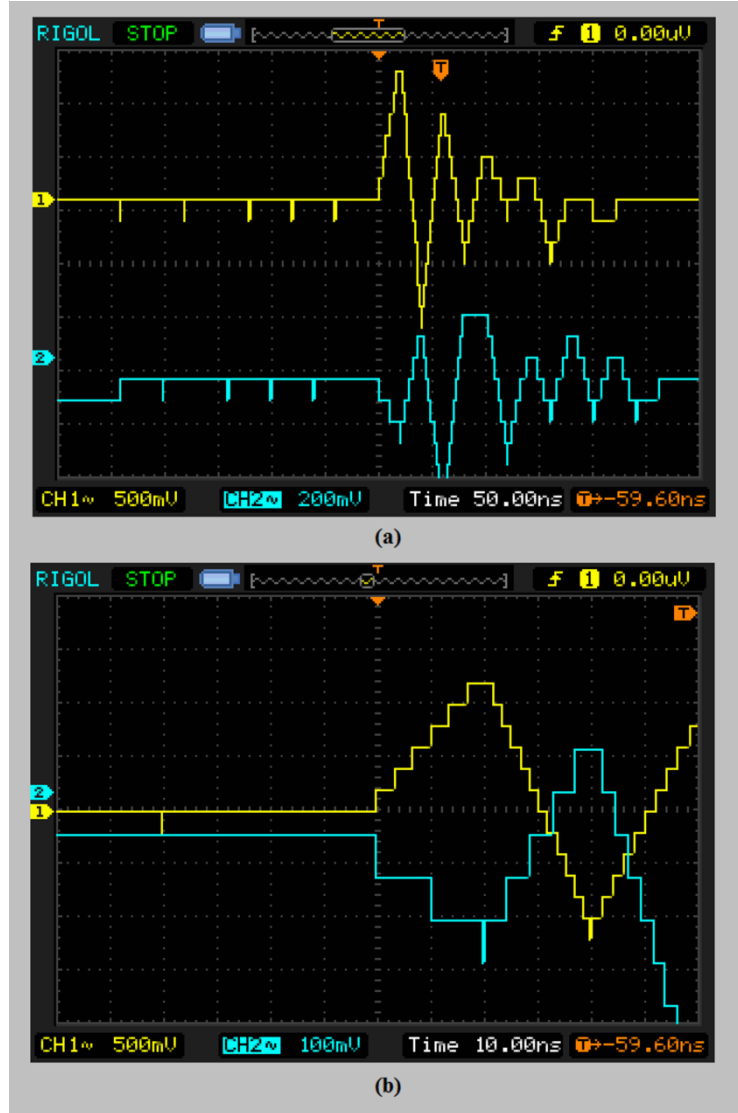
Fig. 10 The spark gap was discharged manually by touching a metal contact for an instant. (a) The Tx (yellow, top) and Rx (blue, bottom) signals generated. Null result, no measurable propagation time delay on air between the Tx and Rx signals in the near-field. The osc probes for this measurement were set both at x1 setting.

 In Figure 10, we measured the signals by briefly short-circuiting the previously charged spark gap of the Wimshurst machine with a metal contact plate. Our 1Gsps digital oscilloscope allowed us to demonstrate an absolute null time delay difference between the Tx and Rx signals. In particular for this measurement shown in Figure 10 to obtain shorter and cleaner signals for comparison, we used a metal plate manually short-circuiting the spark gap and causing a violent discharge, which produced a spark at the contact points. The signal waveforms appeared quantized due to their relatively small strength and very short duration, which was less than 100ns in total.

 Our findings support the results of previous independent researchers [1-5, 7, 8, 9, 10]. They suggest that radio signal fluctuations propagate superluminally, i.e., faster than the speed of light c, in the near-field. This behavior is attributed to the Coulomb longitudinal component contribution in the near-field (i.e., within one wavelength distance) and the non-local nature of Maxwell's displacement

12

current predicted within his theory of electromagnetism, as also analyzed by Heras J. [11]. Our experiments confirm this superluminal behavior. We conducted a novel experiment that differs from previous ones, including Gasser W.'s [5] work, by successfully isolating what we believe to be the longitudinal component of the Coulomb near-field, which is also observed in the Maxwell displacement current of capacitors between their two plates or poles separated by a dielectric layer like air. In contrast to Gasser W.'s experiment, we took special care to align the Tx spark air gap capacitance with the Rx sensor capacitor along their length axis, using laser beam alignment to isolate the longitudinal component of the received signal. Also, we kept the distance as minimal as possible, and the spark signal generated power was much larger, ranging from 30KV at an 8mm spark gap to 70KV at a 30mm spark gap, compared to Gasser W.'s experiment, which produced sparks at only 10KV. Therefore, in our experiment, a much stronger signal was generated and transmitted during our measurements, resulting in a much stronger effect produced. The spark gap height was 1.75m from the ground. Furthermore, we low pass filtered and constrained the bandwidth of our measured signals to minimize any interference from higher frequency harmonics or ghost images that could interfere with the experiment. This ensured that, as much as possible, the direct Tx spark signal was measured, as demonstrated in Fig. 8. When conducting experiments involving the propagation of near-field static Coulomb field fluctuations, it is important to isolate the direct longitudinal air propagating component of the transmitted signal as much as possible, and prevent any far-field transverse electromagnetic waves from interfering with your measurement. To achieve this, a short distance and filtered setup is more suitable. However, such a setup requires more effort to control due to the short propagation time it imposes.

Although the oscilloscope we used had both channels and both grounds fully isolated as stated in its specifications. In order to address and make sure that no substantial signal ghost images were passing through the two isolated channel grounds, we repeated the experiments using a second separated oscilloscope and synchronized the two oscilloscopes together. We found again the same null result as before. A description of the two oscilloscopes setup experiment and a sample of the results can be found in this supplementary material repository here[2].

Next, we present an analysis of the Maxwell theory of electromagnetism that supports the superluminal behavior we observed in the near-field.

3.1 Analysis of Maxwell theory for the near-field propagation speed

Theoretical analysis shows that according to Maxwell's equations, the inhomogeneous wave equation for the Electric Field (E), where (ρ) is the charge density, (J) is the current density, and (c) is the far-field speed of light [2]:

$$\nabla^2 E - \frac{1}{c^2}\frac{\partial^2 E}{\partial t^2} = 4\pi\nabla\rho + \frac{4\pi}{c^2}\frac{\partial J}{\partial t} \tag{2}$$

---

[2] http://tinyurl.com/bddhytvs

13

The longitudinal Electric field solution for a harmonic oscillator dipole source, where (ω) is the angular frequency of the source, (k) is the wave vector, (r) is the distance from the source, and (θ) is the angle reference the dipole:

$$E_r = \frac{2p_o \cos(\theta)}{r^3} e^{i(kr-\omega t)}[1 - i(kr)] \qquad (3)$$

The resultant phase shift of the longitudinal Electric field is therefore: $\theta = kr - Tan^{-1}kr$

- Phase speed formula: $c_{ph} = -ck / \dfrac{\partial \theta}{\partial r}$ $\qquad (4)$

- Group speed formula: $c_g = -c\left[\dfrac{\partial^2 \theta}{\partial r \partial k}\right]^{-1}$ $\qquad (5)$

- Phase speed formula (c_{ph}) : $c_{ph} = -c_o k / \dfrac{\partial \theta}{\partial r}$ $\qquad (6)$

- Group speed formula (c_g): $c_g = -c\left[\dfrac{\partial^2 \theta}{\partial r \partial k}\right]^{-1}$ $\qquad (7)$

- Resultant equations for longitudinal Electric field phase speed, and group speed as a function of the product kr:

$$c_{ph} = c\left(1 + \frac{1}{(kr)^2}\right) \underset{kr\ll 1}{\approx} \frac{c}{(kr)^2} \underset{kr\gg 1}{\approx} c$$

$$c_g = \frac{c\left(1 + (kr)^2\right)^2}{3(kr)^2 + (kr)^4} \underset{kr\ll 1}{\approx} \frac{c_{ph}}{3} \underset{kr\gg 1}{\approx} c \qquad (8)$$

Phase vs Distance   Phase Speed vs Distance   Group Speed vs Distance
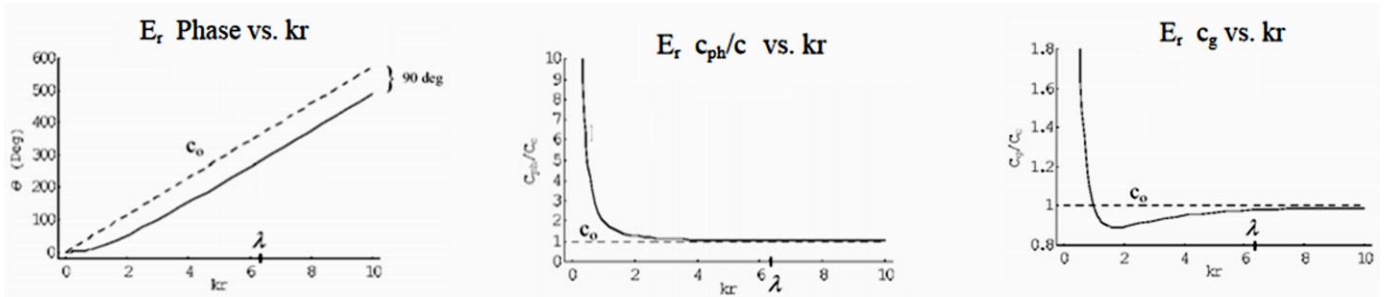

Fig. 11 Equations plots of the longitudinal Electric field E_r, phase speed c_{ph}, and group speed c_g vs. the kr product parameter [2].

14

The results shown in Fig. 11 show that the slope of phase vs. distance curve for the longitudinal Electric field has a minima at the source and becomes linear about one wavelength (λ) from the source. Consequently, since the phase speed and group speed are inversely proportional to the slope of the phase vs. distance curve, they are instantaneous at the source and reduce to the speed of light about one wavelength from the source.

4. Conclusion

We report a null result or negative experiment result for a finite propagation delay of the near-field displacement current of an air capacitor existing between its two poles. Which was previously predicted and also experimentally verified by W. Walker et al. [1-4] in general for propagating longitudinal near-field radio signals, but is also predicted by Maxwell's theory for the non-local nature of the displacement current [11]. We believe that both phenomena, Walker's generalization for superluminal transmission of radio signals in the near-field and Maxwell's theory non-local nature of the displacement current are correlated for the near-field. This experiment has led us to conclude that there is instantaneous or at least superluminal propagation within a 1ns uncertainty of our experiment on the expected 5ns value predicted by the known group speed of light and information speed. Therefore, we have a confidence level of 80% in our results. However, we must note that we were limited by short propagation time of the experimental setup, and the capabilities of the oscilloscope used. In future experiments, it would be beneficial to include a picoseconds time base oscilloscope or other measuring apparatus capable of measuring at the picoseconds scale. It would also simplify the experiment setup and its unknown control parameters effects by using a single giant parallel plates air capacitor, shielded if possible, with its two plates separated at a sufficient distance. By measuring the electric spark discharge signal propagation delay between its plates, we can determine the propagation signal speed of its Coulomb field existing in the air in-between its plates at near-field frequencies. Encouraged by these results, we predict that the research field of superluminality will play a crucial role in explaining some of the unknowns in physics, particularly in quantum theory [12] [13]. This may help to clarify its apparent weirdness and incompatibility with general relativity, and could potentially serve as the missing piece in the puzzle for quantum gravity. We believe that superluminal phenomena warrant further investigation and should not be easily dismissed. There will be both quantum interpretations and electrodynamic interpretations, which may differ. But the point is that in this experiment, information of the spark event arrived at the detector faster than a light speed propagating signal. This experiment clearly shows for the first time that information can be transmitted and received across space faster than light and can be used for superluminal, if not instantaneous, communication of information.

Acknowledgements

Declarations

The authors have no relevant financial or non-financial interests to disclose.
The authors did not receive support from any organization for the submitted work.

References

[1]   W. D. Walker, J. Dual, 'Phase speed of longitudinally oscillating gravitational fields', Edoardo Amaldi conference on gravitational waves, World Scientific Pub., (1997). https://arxiv.org/abs/gr-qc/9706082v2 (accessed March 25, 2023).

[2]   W.D. Walker, Superluminal Electromagnetic and Gravitational Fields Generated in the Nearfield of Dipole Sources, (2006). https://arxiv.org/abs/physics/0603240v1 (accessed January 17, 2024).

[3]   W. D. Walker, 'Experimental evidence of near-field superluminally propagating electromagnetic fields', Vigier III Symposium "Gravitation and Cosmology", Berkeley, California, USA, 21-25, Kluwer Pub., August (2000). https://arxiv.org/abs/physics/0009023v1 (accessed November 27, 2023).

[4]   W.D. Walker, Near-field electromagnetic effects on Einstein special relativity, (2008). https://arxiv.org/abs/physics/0702166 (accessed January 17, 2024).

[5]   W.G. Gasser, Experimental Clarification of Coulomb-Field Propagation Superluminal information transfer confirmed by simple experiment, (2016). http://tinyurl.com/5sc7xtmv (accessed August 22, 2023).

[6]   D.W. Park, G.S. Kil, S.G. Cheon, S.J. Kim, H.K. Cha, Frequency Spectrum Analysis of Electromagnetic Waves Radiated by Electric Discharges, J. Electr. Eng. Technol. 7 (2012) 389–395. doi:10.5370/JEET.2012.7.3.389.

[7]   L. Nanni, Electromagnetic field theory in superluminal spacetime, Indian J. Phys. 2023. (2023) 1–11. doi:10.1007/S12648-023-02747-3.

[8]   L. Nanni, Evanescent waves and superluminal behavior of matter, Https://Doi.Org/10.1142/S0217751X19501410. 34 (2019). doi:10.1142/S0217751X19501410.

[9]   L. Nanni, On photonic tunnelling and the possibility of superluminal transport of electromagnetic energy, Pramana - J. Phys. 97 (2023) 1–9. doi:10.1007/S12043-022-02511-Y/METRICS.

[10]   R. de Sangro, G. Finocchiaro, P. Patteri, M. Piccolo, G. Pizzella, Measuring propagation speed of Coulomb fields, Eur. Phys. J. C. 75 (2015). doi:10.1140/epjc/s10052-015-3355-3.

[11]   J.A. Heras, A formal interpretation of the displacement current and the instantaneous formulation of Maxwell's equations, Am. J. Phys. 79 (2011) 409–416. doi:10.1119/1.3533223.

[12]   A. Dragan, A. Ekert, Quantum principle of relativity, New J. Phys. 22 (2020) 033038. doi:10.1088/1367-2630/AB76F7.

[13]   A. Dragan, K. Dębski, S. Charzyński, K. Turzyński, A. Ekert, Relativity of superluminal observers in 1 + 3 spacetime, Class. Quantum Gravity. 40 (2023) 025013. doi:10.1088/1361-6382/acad60.